The dynamism of salt crust patterns on playas

Joanna M. Nield[1]*, Robert G. Bryant[2], Giles F.S. Wiggs[3], James King[3], David S.G. Thomas[3,4,5], Frank D. Eckardt[4], and Richard Washington[3]

[1]Geography and Environment, University of Southampton, Southampton SO171BJ, UK
[2]Department of Geography, University of Sheffield, Sheffield, South Yorkshire S102TN, UK
[3]School of Geography and the Environment, University of Oxford, Oxford OX13QY, UK
[4]Department of Environmental and Geographical Science, University of Cape Town, Cape Town 7701, South Africa
[5]School of Geography, Archaeology and Environmental Studies,University of the Witwatersrand, Johannesburg 2000, South Africa

ABSTRACT

Playas are common in arid environments and can be major sources of mineral dust that can influence global climate. These landforms typically form crusts that limit evaporation and dust emission, modify surface erosivity and erodibility, and can lead to over prediction or underprediction of (1) dust-emission potential and (2) water and heat fluxes in energy-balance modeling. Through terrestrial laser scanning measurements of part of the Makgadikgadi Pans of Botswana (a Southern Hemisphere playa that emits significant amounts of dust), we show that over weeks, months, and a year, the shapes of these surfaces change considerably (ridge thrusting of >30 mm/week) and can switch among continuous, ridged, and degraded patterns. Ridged pattern development changes the measured aerodynamic roughness of the surface (as much as 3 mm/week). The dynamic nature of these crusted surfaces must be accounted for in dust entrainment and moisture balance formulae to improve regional and global climate models.

INTRODUCTION

Playas are common landforms in arid regions and are one of the biggest sources of mineral dust emission (Washington et al., 2003; Prospero et al., 2002). They contribute to surface energy balances by modifying moisture and heat fluxes in the atmosphere (Bryant and Rainey, 2002). There is uncertainty as to how much playas contribute to dust emissions (Sweeney et al., 2011) and the extent to which they influence the hydrological budget, because when the water table is shallow, a protective and often heterogeneous mineral crust is typically formed (Reynolds et al., 2007). These crusts can form polygonal patterns that may be smooth and continuous, limiting subsurface exposure, or ridged and cracked, enabling unregulated exchange between surface and subsurface processes.

Uncertainty in dust emission predictions (flux and location) stems from three main controls on crust patterns. (1) Crusts influence the availability of surface material, which varies depending on crust moisture, type, and thickness (Nickling, 1984). (2) The salt chemistry and changes in moisture may result in the formation of weak, low-bulk-density sediment (mineral grains plus salt crystal; fluff), thereby increasing the supply of potentially emissive material (Reynolds et al., 2007), particularly on sulfate-rich playas (Buck et al., 2011). (3) As polygon ridges grow and degrade over time, they alter surface roughness and therefore the erodibility of the surface and erosivity of the wind through modifications to aerodynamic roughness (z_o), a key parameter in modeling dust-emission potential (Raupach et al., 1993; Marticorena and Bergametti, 1995).

*E-mail: J.Nield@soton.ac.uk

This paper assesses surface moisture, aerodynamic roughness, and crust pattern change on a large playa (Sua Pan) in Botswana over weeks, months, and one year. We first introduce the surface variability, and then use Fourier transforms to assess how surface patterns develop over time, ultimately linking surface change to atmospheric and subsurface controls through a conceptual model that identifies trajectories in crust patterning.

SITE LOCATION AND METHODS

Investigations were undertaken during August 2011 and August and September 2012 at 6 locations (sites L5, J11, D10, G6, I4, B7) on Sua Pan within a study area of 144 km^2 centered at 20.5754°S, 25.959°E. Sua Pan is part of the 3400 km^2 Makgadikgadi complex in Botswana. This playa undergoes ephemeral flooding and its surface consists of a polygonal salt crust that is predominantly halite, thenardite, and trona (Eckardt et al., 2008). The surface includes freshly formed crust with no or low topographic perturbations (continuous), well-formed polygon ridges (ridged), older broken, deflated ridges (degraded), or a mix of these three surfaces.

The surface elevations of the crust were measured using a Leica Scanstation terrestrial laser scanner (TLS) and converted to 100 m^2 digital elevation models of 1-cm-grid resolution following the methods of Nield et al. (2013). Registration errors between monthly and weekly scans were <2 mm. Locations between years were registered using a differential GPS survey. Ridge height, width, and spacing were calculated by linearly detrending 1-cm-spaced transects and identifying positive height deviations (Nield et al., 2013). Two-dimensional Fourier transforms (following the method of Perron et al., 2008) were used to calculate radial frequencies and corresponding ridge spacings, which were normalized using the flat surface spectra (site L5 in 2011). Water-table depth was measured using a dipwell in 2 m wells. Relative surface moisture was calculated at each site using the mean intensity of the TLS return signal collected within a 2 m^2 area at a distance of 12.5 m, normalized by the wettest site (site L5 in 2011), following the methods of Nield et al. (2014). High values indicate drier surfaces.

Detection of surface moisture on the entire playa between 2000 and 2012 was based on normalized difference water index (NDWI) data extracted from Moderate Resolution Imaging Spectroradiometer (MODIS) MOD/MYD09A1 8 day data (500 m resolution) (Gao, 1996; Leon and Cohen, 2012). NDWI threshold values were validated using field observations of surface condition (i.e., flooded, moist, and dry) from various basin locations along with high-resolution remote sensing data (e.g., Advanced Spaceborne Thermal Emission and Reflection Radiometer, ASTER; Landsat). Processed data were consolidated to provide long-term and annual surface flood frequency data (F_f; Figs. 1A–1C), and, for the 2010–2012 hydrological years, 8 day NDWI data were extracted for each study site (Fig. 1D).

Values of z_o were calculated using 2 weeks of easterly wind speeds measured at 0.25 m, 0.47 m, 0.89 m, and 1.68 m with Vector Instruments cup anemometers (A-100R), averaged over 1 min intervals following standard law of the wall profile methods. Measurements below 3 m s^{-1} or with R^2 values below 0.98 were discarded (Bauer et al., 1992).

SURFACE MOISTURE OBSERVATIONS

Surface water varied annually as a function of elevation, with topographically lower sites in the east (sites L5 and J11) being submerged more frequently over a 10 yr period than sites in the central (sites G6, I4) and western (sites D10, B7) areas (Fig. 1A). In the 2010–2011 wet season, prior to field measurements (Fig. 1B), only the western sites (D10, B7) remained relatively dry (Fig. 1D), while during the 2011–2012 wet season (Fig. 1C), only the center (G6, I4) underwent prolonged flooding (Fig. 1D). TLS moisture measurements (Table 1) indicated drying (higher val-

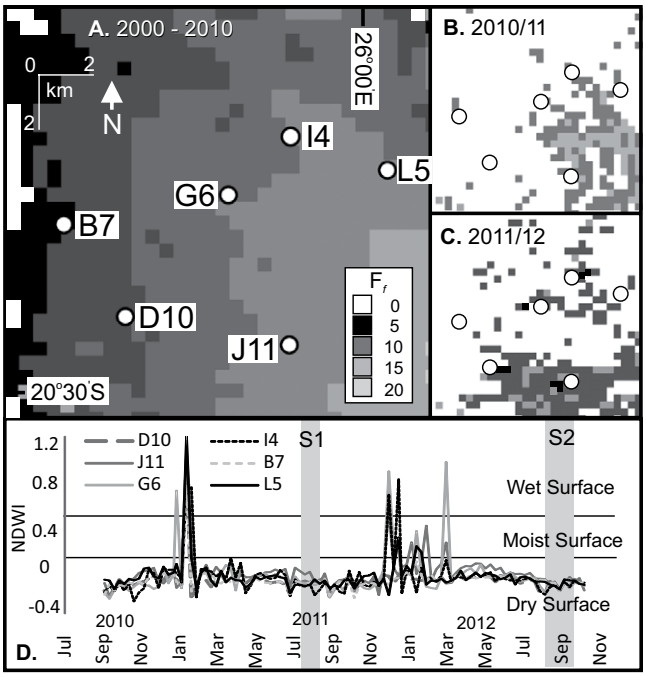

Figure 1. Surface moisture trends (flood frequency, F_f) assessed by the Moderate Resolution Imaging Spectroradiometer. A: 10 yr of data between 2000 and 2010 (scale is fraction of time between 0% and 20% of time that the playa was inundated). B: Data for year prior to ground measurements (2010–2011). C: Data for year between ground measurements (2011–2012) using the same scale. D: Temporal sequence of surface moisture within 0.25 km² area surrounding each site. S1 and S2 indicate study periods; L5, J11, D10, G6, I4, and B7 indicate study sites. NDWI—normalized difference water index.

TABLE 1. PHYSICAL MEASUREMENTS AND CALCULATED z_o VALUES FOR EACH SITE AND TIME PERIOD

Site	Date (dd/m/yyyy)	Surface pattern	z_o (mm)		Water table	Normalized surface moisture		Ridge height (mm)			Ridge (m)	
			μ	σ	(m)	TLS	MODIS	μ	max	σ	width	spacing
L5	20/8/2011	continuous	0.07	0.06	0.52	1.00	–0.13	0.8	6.8	0.4	0.035	0.056
	03/8/2012	continuous	0.46	0.30	0.745	1.06	–0.112	8.1	44.1	5.1	0.181	0.270
	12/8/2012	ridged	4.25	5.02	0.785	-	–0.109	13.8	58.7	7.5	0.187	0.310
	14/9/2012	ridged	5.60	5.90	0.905	-	–0.190	18.4	61.6	10.0	0.181	0.325
	17/9/2012	ridged	6.93	7.45	0.905	-	–0.12	17.6	60.9	9.9	0.174	0.309
	26/9/2012	ridged	5.00	5.98	0.78	-	–0.14	17.6	70.0	9.9	0.170	0.301
J11	22/8/2011	continuous	0.59	0.49	0.77	1.05	–0.125	4.3	21.2	2.8	0.078	0.126
	09/8/2012	ridged	2.45	1.20	>0.68	1.11	–0.084	21.9	101.5	14.1	0.229	0.384
	21/9/2012	ridged	3.27	1.31	0.635	-	–0.130	23.3	90.3	15.1	0.227	0.382
D10	18/8/2011	ridged	3.57	1.84	1.54	1.13	–0.1	19.7	63.2	10.8	0.237	0.383
	05/8/2012	ridged	2.16	0.94	1.755	1.16	–0.111	26.0	96.6	14.5	0.269	0.452
	19/9/2012	ridged	2.97	1.24	1.815	-	–0.11	29.9	93.8	15.8	0.275	0.472
G6	09/8/2011	degraded	2.63	1.18	1.31	1.14	–0.141	17.1	63.9	8.8	0.126	0.222
	01/8/2012	degraded	0.71	0.51	1.745	1.13	–0.083	8.3	64.5	6.8	0.130	0.223
	20/9/2012	degraded	3.55	4.59	1.845	-	–0.09	8.4	69.1	7.0	0.124	0.219
I4	21/8/2011	degraded	2.63	1.58	-	1.13	–0.184	12.0	52.1	7.0	0.074	0.148
	04/8/2012	mixed	0.65	0.42	1.105	1.10	–0.104	11.0	62.7	7.4	0.180	0.294
	23/9/2012	ridged	2.70	1.10	1.105	-	–0.11	16.7	66.5	9.7	0.178	0.310
B7	15/8/2011	mixed	0.62	0.36	1.02	1.08	–0.086	5.5	42.7	4.1	0.077	0.112
	02/8/2012	mixed	1.26	0.70	>0.937	1.10	–0.099	16.8	90.7	14.6	0.248	0.376
	18/9/2012	mixed	6.97	7.29	0.835	-	–0.190	24.5	99.3	17.1	0.291	0.469

Note: z_o—aerodynamic roughness; μ—mean; σ—standard deviation; TLS—terrestrial laser scanner; MODIS—Moderate Resolution Imaging Spectroradiometer. Dashes indicate no data.

ues) on surfaces that did not undergo prolonged flooding in 2011–2012 (L5, B7, J11, D10), and a slight increase (lower values; 1%–3%) in surface moisture at flooded sites (G6, I4).

RIDGED PATTERN DEVELOPMENT

The combination of a high water table and flooding in 2011 reset the surface and enabled a flat, continuous crust to develop on the northeastern section of the playa (L5). After the wet season in 2011–2012, when no significant flooding occurred (Fig. 1D), the surface dried enough to initiate ridge formation (Fig. 2A). During 3–12 August 2012 (Table 1), ridge crests were thrust up by as much as 30 mm (Fig. 2E). While the mean surface change was 0.44 mm/day (Fig. 2H), most growth was near the ridge peaks, and the interridge areas remained at the same elevation, as indicated by the asymmetric growth distribution with a peak at zero and a tail extending to 2 mm/day. This initial growth period slowed in the latter part of August and early September (mean rate of 0.23 mm/day between 12 August and 14 September; Fig. 2G). By late September (17–26 September), the growth distribution became more symmetrical (Fig. 2I), ridges had reached their maximum stability, and heights began to reduce (–0.05 mm/day). Fourier transform spectra capture this pattern of ridge growth and decline and indicate increased persistence of ridge spacing in the 200–300 mm region throughout August and early September, and a slight decline in mid to late September (Fig. 2D).

SPATIAL AND TEMPORAL VARIABILITY OF CRUST PATTERNS

In a manner similar to that of the northeast crust at site L5, high levels of surface moisture toward the southeast (site J11; Fig. 3A) in 2010–2011 (Fig. 1D) reset the surface and formed a continuous crust prior to our measurements. The small moisture inputs and a diminished peak in surface water between August 2011 and August 2012 (Fig. 1D) were not enough to reset this surface between our measurement periods, but instead assisted in the development of a fast-forming, distinctive, and widely spaced ridged pattern in 2012 (similar to site D10).

In the drier southwest section of the playa (site D10), a well-defined ridged pattern continued to grow between August 2011 and August 2012. This growth extended the dominance of larger spaced (600 mm) ridges (Fig. 3B) because the playa did not undergo any substantial flooding during the wet seasons in 2010–2011 or 2011–2012 (Fig. 1D). The mixed pattern on the western side of the study area (site B7; Fig. 3E) followed a similar temporal trend in ridge development, but it had fewer ridges initially because it had more extensive flooding in 2010–2011 (Fig. 1D) and had a shallower water table (0.835 m and 1.815 m for sites B7 and D10, respectively; Table 1).

The smooth, degraded surfaces in the central areas of the playa (sites G6 and I4; Figs. 3C and 3D) indicated strong, smaller ridge spacing (between 100 and 300 mm) initially. This topography became muted after the substantial flooding around site G6 (Fig. 1D) during the 2011–2012 wet season, or transitioned through a mixed phase to a well-developed ridged pattern where standing water was not consistently present as at site I4 (Fig. 3D). The surface at G6 did not form typical polygonal ridges during 2012, but instead there was a general swelling in elevation of the entire surface. This swelling was evident to a lesser extent at the drier surface (site I4) and appears to be related to the thickness of the degraded crust, which limits capillary action and subsurface moisture exchange (Nickling and Ecclestone, 1981). Vehicle tracks on the surface (site I4; Fig. 3D) followed the crust development trajectory of degraded to

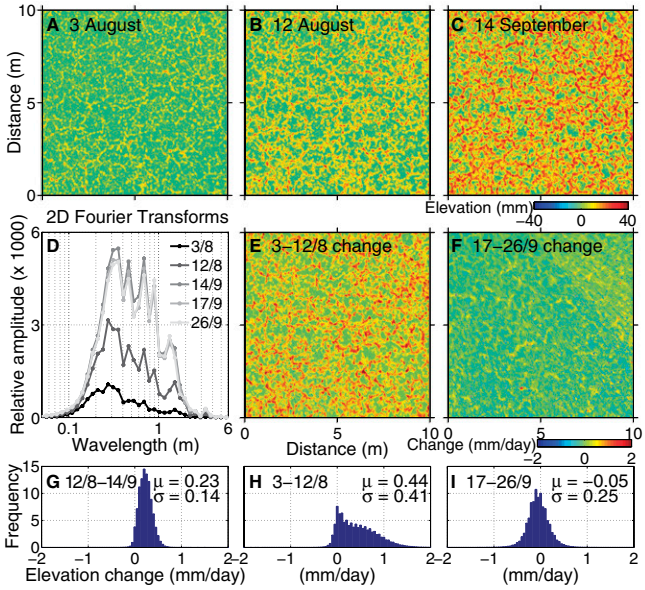

Figure 2. A–C: Examples of planform surfaces at study site L5 depicting ridge development. Colors indicate surface elevation above (red) and below (blue) mean height of 3 August 2012 surface. D: Relative amplitude of two-dimensional (2-D) Fourier transform wavelengths for each surface measurement. E, F: Surface change over 9 days (3–12 August, 17–26 September 2012). G–I: Frequency of elevation change (mean and standard deviations indicated by μ and σ, respectively, in mm/day), 12 August through 14 September, 3–12 August, and 17–26 September 2012.

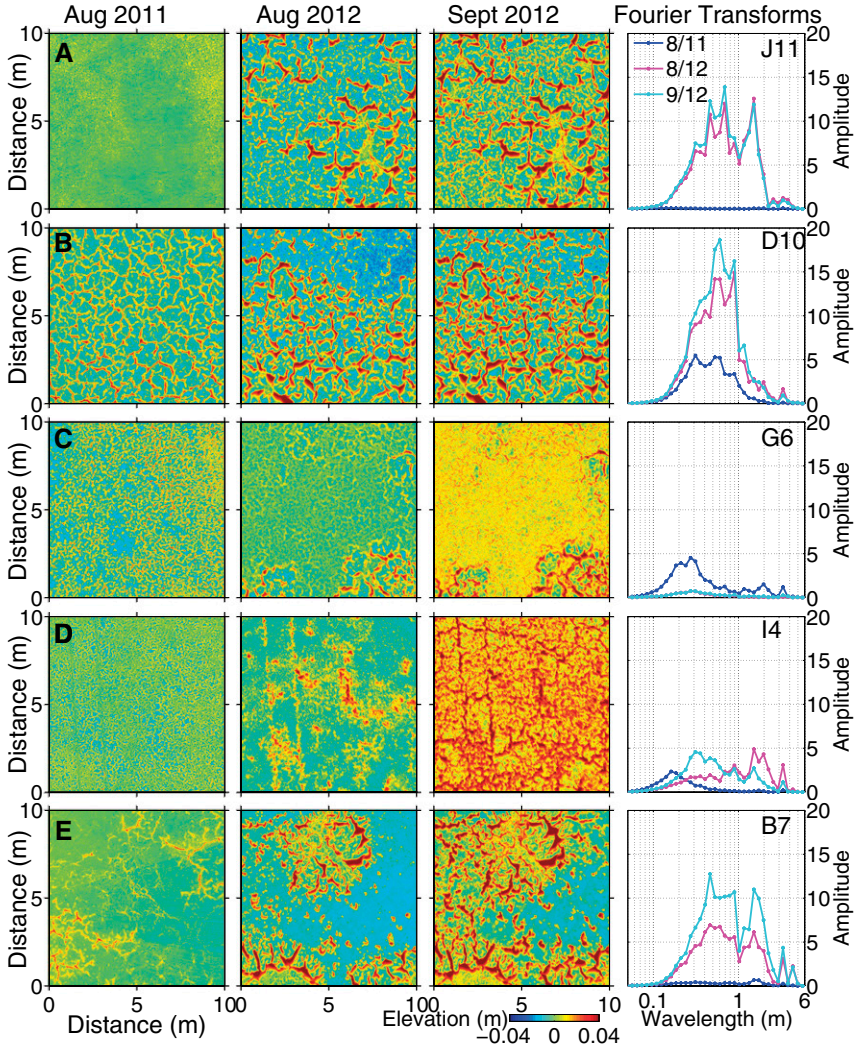

Figure 3. Examples of surfaces in 2011 and subsequent patterns in 2012. Colors indicate surface elevation above (red) and below (blue) mean height for each year in August. Relative amplitudes of two-dimensional Fourier transform wavelengths for each pattern are indicated in right column, normalized to the spectra from the flat surface at site L5 in 2011.

mixed to ridged, and highlight the importance of small-scale topography in crust pattern development. During the wet season in 2011–2012, it is likely that these topographically depressed areas preferentially ponded water, initializing earlier ridge development in 2012. The forcing by moisture inverted the crust pattern, resulting in vehicle tracks becoming topographically positive after the wet season (Fig. 3D).

TEMPORAL VARIABILITY OF z_o

In general, z_o values (Table 1) across the study site relate to ridge dimensions, and were greater on surfaces with larger element heights (Nield et al., 2013). Temporally, z_o values increased as the surfaces transitioned from flatter to ridged patterns. The higher resolution measurement sequence undertaken at site L5 (Table 1) demonstrates the rapidity at which the formation of a ridged pattern can induce an order of magnitude change in z_o, increasing from 0.46 mm to 4.25 mm in 9 days (3–12 August 2012). This change in z_o occurred as a result of a growth in the mean ridge height from 8.1 mm to 13.8 mm over the same period.

FEEDBACKS, CONROLS, AND DRIVERS OF SALT CRUST PATTERNING

Using high-resolution TLS sequences (days and millimeters), we build upon the conceptual postulations of Krinsley (1970), where polygonal ridge thrusting is driven by efflorescence. We find that ridge development (Fig. 4A; sites L5 and J11 trajectories) is a complex process likely controlled by flooding and interactions among subsurface, surface, and atmospheric moisture exchange (Groeneveld et al., 2010). Positive feedback accelerates ridge development because higher, exposed ridges increase evaporation, salt phase change, and thrusting. Over time, negative feedback diminishes ridge growth (Fig. 4B; site G6 trajectory) because ridges may collapse, either through structural weaknesses or mechanical and chemical breakdown by wind and/or rain. Under extreme external events such as flooding from river flow, rainfall, or upwelling, the surface may be reset at any stage of the formation-degradation cycle (Fig. 4C; site I4 trajectory). Continuous crusts in our conceptual model will have low evaporation and dust-emission rates, ridged crusts will have high evaporation rates but low dust-emission rates, and degraded crusts will have high dust-emission rates but lower evaporation rates than other crust types. Water-table depth, salt chemistry, and antecedent conditions are important controls on the extent to which a surface may progress through different pattern phases. For example, concentrations of thenardite and a high water table may increase the development of ridges and fluffy dust-emitting sediment, or interlocking halite crystals may decrease the availability of dust sediment (Buck et al., 2011).

Chemical salt segregation within ridged and flat surfaces may also influence dust emissivity. The resulting surface patterns modify z_o (Table 1) and therefore have important implications for dust emission and evaporation rates because z_o is a component of both dust entrainment thresholds and turbulent heat fluxes (Deol et al., 2012; Bryant, 2013). For example, the increase in z_o over 9 days in August could result in an increase in shear velocity threshold by as much as 350% using the Marticorena and Bergametti (1995) scheme, which could lead to an overprediction in dust emission modeling.

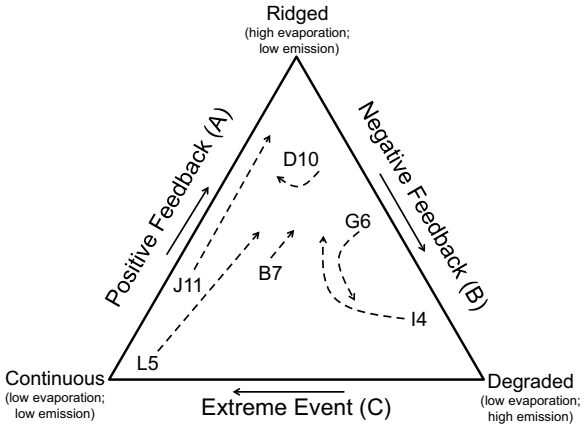

Figure 4. Conceptual diagram linking salt-crust pattern change to feedbacks and extreme events. A: Positive feedback controlled by subsurface, surface, and atmospheric processes, which over time lead to ridge development. B: Negative feedback controlled by atmospheric processes which, over time, together with wind and/or rain, lead to crust degradation. C: Extreme flooding events controlled by subsurface and atmospheric processes reset the crust. Dashed lines indicate the trajectories of each surface between August 2011 and September 2012.

CONCLUSIONS

This work shows that detailed time series data on surface microtopography and groundwater and/or surface water status are required to fully characterize crust pattern formation and/or degradation. Our data suggest the following.

1. Ridge heights increase over time due to positive feedbacks between atmospheric and subsurface processes, unless external controls reset the surface.

2. Over time, ridge growth rates decrease due to negative feedbacks, limiting atmospheric and subsurface interactions.

3. On young crusts, ridge initiation and growth can occur quickly (>30 mm/week), changing the erosion potential by increasing z_o.

4. Sediment supply and availability increase as the surface dries out, becomes cracked, and exposes freshly made, low-density, fluffy sediment.

This paper gives the first indication of salt-crust pattern variability, both temporally and spatially, for a major dust hot spot (Gillette, 1997), one of the largest paleolakes in the Southern Hemisphere. Ultimately, we show that it is important to include parameterization of salt-crust pattern dynamics (at the level of detail that we provide here) within climate models to better account for changes in water balance, dust entrainment, sediment availability, and salt accumulation in the geological record.

ACKNOWLEDGMENTS

This study was funded by the Natural Environment Research Council (NE/H021841/1), the World University Network, and a Southampton SIRDF (Strategic Interdisciplinary Research Development Funds) grant. We thank the Botswana Ministry of Environment, Wildlife, and Tourism (permit EWT 8/36/4 XIV), Botswana Ash (Pty) Ltd., W.G. Nickling, the reviewers, and Iridis Southampton Computing Facility.

REFERENCES CITED

Bauer, B.O., Sherman, D.J., and Wolcott, J.F., 1992, Sources of uncertainty in shear-stress and roughness length estimates derived from velocity profiles: Professional Geographer, v. 44, p. 453–464, doi:10.1111/j.0033-0124.1992.00453.x.

Bryant, R.G., 2013, Recent advances in our understanding of dust source emission processes: Progress in Physical Geography, v. 37, p. 397–421, doi:10.1177/0309133313479391.

Bryant, R.G., and Rainey, M.P., 2002, Investigation of flood inundation on playas within the Zone of Chotts, using a time-series of AVHRR: Remote Sensing of Environment, v. 82, p. 360–375, doi:10.1016/S0034-4257(02)00053-6.

Buck, B.J., King, J., and Etyemezian, V., 2011, Effects of salt mineralogy on dust emissions, Salton Sea, California: Soil Science Society of America Journal, v. 75, p. 1971–1985, doi:10.2136/sssaj2011.0049.

Deol, P., Heitman, J., Amoozegar, A., Ren, T., and Horton, R., 2012, Quantifying nonisothermal subsurface soil water evaporation: Water Resources Research, v. 48, W11503, doi:10.1029/2012WR012516.

Eckardt, F.D., Bryant, R.G., McCulloch, G., Spiro, B., and Wood, W.W., 2008, The hydrochemistry of a semi-arid pan basin case study: Sua Pan, Makgadikgadi, Botswana: Applied Geochemistry, v. 23, p. 1563–1580, doi:10.1016/j.apgeochem.2007.12.033.

Gao, B.C., 1996, NDWI—A normalized difference water index for remote sensing of vegetation liquid water from space: Remote Sensing of Environment, v. 58, p. 257–266, doi:10.1016/S0034-4257(96)00067-3.

Gillette, D.A., 1997, Physical mechanisms explaining the existence of 'hot spots' of dust emitting source regions, *in* Hoyningen-Huene, W., and Tetzlaff, G., eds., Sediment and aerosol: Leipzig, Germany, Alfred-Wegener-Stiftung, p. 27–31.

Groeneveld, D.P., Huntington, J.L., and Barz, D.D., 2010, Floating brine crusts, reduction of evaporation and possible replacement of fresh water to control dust from Owens Lake bed, California: Journal of Hydrology, v. 392, p. 211–218, doi:10.1016/j.jhydrol.2010.08.010.

Krinsley, D.B., 1970, A geomorphological and paleoclimatological study of the playas of Iran. Part 1: Washington, D.C., U.S. Geological Survey for the Air Force Cambridge Research Laboratories, Final Scientific Report CP 70–800, 356 p.

Leon, J.X., and Cohen, T.J., 2012, An improved bathymetric model for the modern and palaeo Lake Eyre: Geomorphology, v. 173–174, p. 69–79, doi:10.1016/j.geomorph.2012.05.029.

Marticorena, B., and Bergametti, G., 1995, Modeling the atmospheric dust cycle: 1. Design of a soil-derived dust emission scheme: Journal of Geophysical Research, v. 100, p. 16415–16430, doi:10.1029/95JD00690.

Nickling, W.G., 1984, The stabilizing role of bonding agents on the entrainment of sediment by wind: Sedimentology, v. 31, p. 111–117, doi:10.1111/j.1365-3091.1984.tb00726.x.

Nickling, W.G., and Ecclestone, M., 1981, The effects of soluble salts on the threshold shear velocity of fine sand: Sedimentology, v. 28, p. 505–510, doi:10.1111/j.1365-3091.1981.tb01698.x.

Nield, J.M., et al., 2013, Estimating aerodynamic roughness over complex surface terrain: Journal of Geophysical Research, v. 118, p. 12948–12961, doi:10.1002/2013JD020632.

Nield, J.M., King, J., and Jacobs, B., 2014, Detecting surface moisture in aeolian environments using terrestrial laser scanning: Aeolian Research, v. 12, p. 9–17, doi:10.1016/j.aeolia.2013.10.006.

Perron, J.T., Kirchner, J.W., and Dietrich, W.E., 2008, Spectral signatures of characteristic spatial scales and nonfractal structure in landscapes: Journal of Geophysical Research, v. 113, F04003, doi:10.1029/2007JF000866.

Prospero, J.M., Ginoux, P., Torres, O., Nicholson, S.E., and Gill, T.E., 2002, Environmental characterization of global sources of atmospheric soil dust identified with the Nimbus 7 Total Ozone Mapping Spectrometer (TOMS) absorbing aerosol product: Reviews of Geophysics, v. 40, p. 2-1–2-31, doi:10.1029/2000RG000095.

Raupach, M.R., Gillette, D.A., and Leys, J.F., 1993, The effect of roughness elements on wind erosion threshold: Journal of Geophysical Research, v. 98, p. 3023–3029, doi:10.1029/92JD01922.

Reynolds, R.L., Yount, J.C., Reheis, M., Goldstein, H., Chavez, P., Fulton, R., Whitney, J., Fuller, C., and Forester, R.M., 2007, Dust emission from wet and dry playas in the Mojave desert, USA: Earth Surface Processes and Landforms, v. 32, p. 1811–1827, doi:10.1002/esp.1515.

Sweeney, M., McDonald, E., and Etyemezian, V., 2011, Quantifying dust emissions from desert landforms, eastern Mojave Desert, USA: Geomorphology, v. 135, p. 21–34, doi:10.1016/j.geomorph.2011.07.022.

Washington, R., Todd, M., Middleton, N.J., and Goudie, A.S., 2003, Dust-storm source areas determined by the total ozone monitoring spectrometer and surface observations: Association of American Geographers Annals, v. 93, p. 297–313, doi:10.1111/1467-8306.9302003.

Manuscript received 13 August 2014
Revised manuscript received 16 October 2014
Manuscript accepted 18 October 2014

Printed in USA